JACS
JOURNAL OF THE AMERICAN CHEMICAL SOCIETY

ARTICLE

pubs.acs.org/JACS

Conserved Tyr223$^{5.58}$ Plays Different Roles in the Activation and G-Protein Interaction of Rhodopsin

Matthias Elgeti,[*,†,∥] Roman Kazmin,[†,∥] Martin Heck,[†] Takefumi Morizumi,[†,⊥] Eglof Ritter,[†] Patrick Scheerer,[†] Oliver P. Ernst,[†,±] Friedrich Siebert,[†,‡,¶] Klaus Peter Hofmann,[*,†,§] and Franz J. Bartl[*,†,§]

[†]Institut für Medizinische Physik und Biophysik, Charité—Universitätsmedizin Berlin, Berlin, Germany

[‡]Max-Volmer-Laboratorium für Biophysikalische Chemie, Technische Universität Berlin, Berlin, Germany

[§]Zentrum für Biophysik und Bioinformatik, Humboldt-Universität zu Berlin, Berlin, Germany

Supporting Information

ABSTRACT: Rhodopsin, a seven transmembrane helix (TM) receptor, binds its ligand 11-*cis*-retinal via a protonated Schiff base. Coupling to the G-protein transducin (G_t) occurs after light-induced *cis*/*trans*-retinal isomerization, which leads through photoproducts into a sequence of metarhodopsin (Meta) states: Meta I ⇌ Meta IIa ⇌ Meta IIb ⇌ Meta IIbH$^+$. The structural changes behind this three-step activation scheme are mediated by microswitch domains consisting of conserved amino acids. Here we focus on Tyr223$^{5.58}$ as part of the Y$^{5.58}$X$_7$K(R)$^{5.66}$ motif. Mutation to Ala, Phe, or Glu results in specific impairments of G_t-activation measured by intrinsic G_t fluorescence. UV−vis/FTIR spectroscopy of rhodopsin and its complex with a C-terminal $G_t\alpha$ peptide allows the assignment of these deficiencies to specific steps in the activation path. Effects of mutation occur already in Meta I but do not directly influence deprotonation of the Schiff base during formation of Meta IIa. Absence of the whole phenol ring (Y223A) allows the activating motion of TM6 in Meta IIb but impairs the coupling to G_t. When only the hydroxyl group is lacking (Y223F), Meta IIb does not accumulate, but the activity toward G_t remains substantial. From the FTIR features of Meta IIbH$^+$ we conclude that proton uptake to Glu134$^{3.49}$ is mandatory for Tyr223$^{5.58}$ to engage in the interaction with the key player Arg135$^{3.50}$ predicted by X-ray analysis. This polar interaction is partially recovered in Y223E, explaining its relatively high activity. Only the phenol side chain of tyrosine provides all characteristics for accumulation of the active state and G-protein activation.

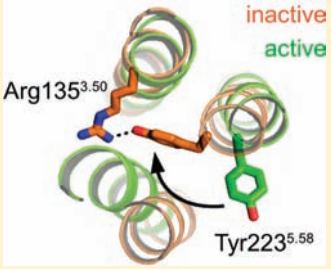

INTRODUCTION

Rhodopsin, the photoreceptor of the vertebrate rod cell, is the archetype of family A G-protein coupled receptors (GPCRs), which receive signals from a variety of ligands.[1] GPCRs are a subgroup of the membrane proteins with seven transmembrane helix (TM) structure. Rhodopsin is a special case, since both the active and inactive state of the receptor harbor the retinal ligand bound via a covalent Schiff base linkage between the retinal aldehyde group and the side chain of Lys296$^{7.43}$ (with Ballesteros/Weinstein numbering superscripted[2]). In the inactive ground state the Schiff base is protonated and the retinal is in its 11-*cis* configuration. Light absorption triggers retinal isomerization and converts the inverse agonist 11-*cis*-retinal into the *all-trans*-retinal agonist. Through fast intermediates and the still inactive metarhodopsin (Meta) I, the active Meta II state is formed, in which the Schiff base is deprotonated. Meta II binds and activates the G-protein transducin (G_t).

In all GPCRs, the sequence of amino acids exhibits several conserved key residues, which form functional domains within the protein structure.[3,4] The most prominent ones are highlighted in the dark state crystal structure of rhodopsin in Figure 1A. It is assumed that these domains act as "microswitches" that change from an inactive to an active conformation in the course of receptor activation.[5] In the dark ground state of rhodopsin, all of these switches are inactive, thereby preventing spontaneous receptor activation. The so-called "ionic lock" is located in the cytoplasmic domain of the receptor and connects two helices via an extended hydrogen-bond network between Arg135$^{3.50}$ (located in the highly conserved (D)ERY-motif in TM3) and Glu247$^{6.30}$ and Thr251$^{6.34}$ in TM6 (Figure 1A,B).[6,7] The Arg135$^{3.50}$ side chain is further stabilized by an intrahelical salt bridge to Glu134$^{3.49}$. Figure 1C depicts the active conformation of the cytoplasmic surface, as found in the available crystal structures of rhodopsin's active states. Spectroscopic and structural investigations suggest that light-activated rhodopsin, ligand-free opsin at low pH (so-called Ops*), and the reversibly formed Meta II in all-*trans*-retinal soaked opsin crystals[8] exhibit similar structures with respect to the cytoplasmic surface.[9,10] In the crystal structure of Ops*, the interaction between Arg135$^{3.50}$ and Glu134$^{3.49}$ is broken and replaced by a new hydrogen bond between the side chains of Tyr223$^{5.58}$ and Arg135$^{3.50}$, while Glu247$^{6.30}$ and Thr251$^{6.34}$ are now coupled to Lys231$^{5.66}$ in TM5.[11] The altered interaction pattern is accompanied by an outward tilt of TM6 by about 6 Å and a movement of TM5 toward TM6 by 2 Å, as indicated by the arrows in Figure 1C. The resulting cleft involving TM3, TM5, and TM6 and the interaction between

Received: February 1, 2011
Published: April 20, 2011

dx.doi.org/10.1021/ja200545n | *J. Am. Chem. Soc.* 2011, 133, 7159–7165

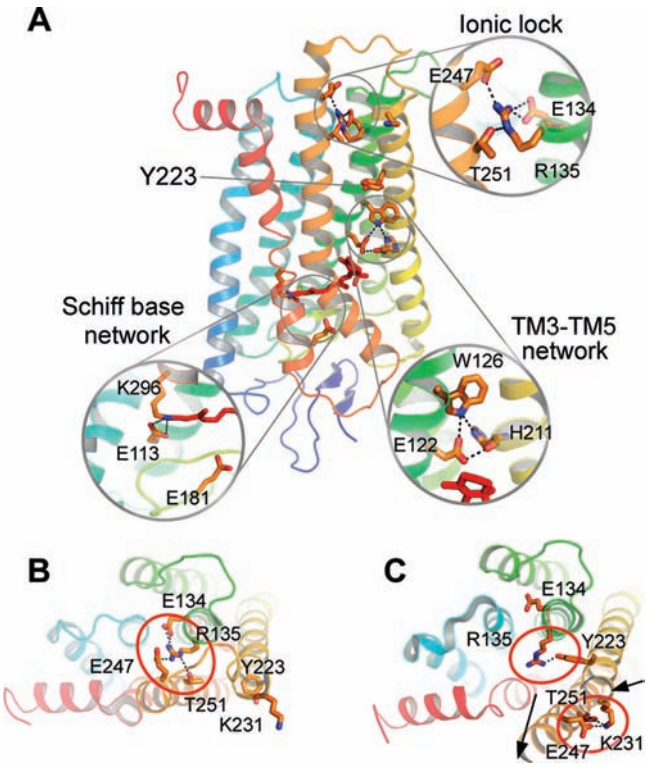

Figure 1. Rhodopsin functional domains and ionic lock. (A) Side view of rhodopsin dark ground state (PDB ID: 1GZM[6]) with helices 1−8 colored blue to red. Side chains of key amino acids that are part of functional domains are highlighted in orange. Three domains of special interest in this study are scaled up: The Schiff base network is stabilized by a complex counterion consisting of Glu113$^{3.28}$; the TM3/TM5 network consists mainly of Glu122$^{3.37}$, Trp126$^{3.41}$, and His211$^{5.46}$ and stabilizes the dark state position of TM5; and the ionic lock is constituted by Arg135$^{3.50}$ and several surrounding groups (Glu134$^{3.49}$, Glu247$^{6.30}$, and Thr251$^{6.34}$) fixing its position and preventing TM6 from outward movement. (B) Top view of the cytoplasmic surface of dark state rhodopsin depicting the inactive conformation of the ionic lock (cf. A). (C) Top view of the structure of ligand-free opsin (PDB ID: 3CAP[11]) representing the active conformation of the ionic lock. Arg135$^{3.50}$ binds to Tyr223$^{5.58}$ via hydrogen bond, and Glu247$^{6.30}$ and Thr251$^{6.34}$ build up new linkages to Lys231$^{5.66}$ from TM5, thereby stabilizing the new arrangement of TM3/TM5 and TM6.

Scheme 1

$$\text{Meta I} \rightleftharpoons \text{Meta IIa} \rightleftharpoons \text{Meta IIb} \rightleftharpoons \text{Meta IIbH}^{+}$$

Arg135$^{3.50}$ and Tyr223$^{5.58}$ at its base constitutes the binding site for the G_t α-subunit and is thus thought to be the crucial structural element of the active receptor when it catalyzes GDP-GTP exchange in the G-protein nucleotide binding pocket.[12−15]

Meta II is the photoproduct that couples to the G-protein.[16] The UV−vis absorption maximum is shifted from 500 nm in dark state rhodopsin to 380 nm in Meta II due to the deprotonation of the retinal Schiff base.[17] At low temperature one observes the pH-dependent equilibrium of Meta II with its inactive precursor Meta I, which is favored at high pH. More recently, kinetic and spectroscopic investigations identified several Meta II subspecies which are populated above 10 °C. The whole process can be arranged in a rapid (millisecond) sequence of conformational substates of Meta II (termed Meta IIa, Meta IIb, and Meta IIbH$^+$, respectively) developing from the inactive precursor Meta I (Scheme 1).[18]

The equilibrium of Meta states, equivalent to the conformational equilibrium of diffusible ligand activated GPCRs[4,19] persists for minutes until eventually the Schiff base hydrolyzes to yield opsin and free *all-trans*-retinal.[20] During this time, increasing temperature depletes the relative amount of Meta I, whereas Meta IIa and Meta IIb accumulate. In Meta I, the counterion of the retinylidene Schiff base shifts from Glu113$^{3.28}$ to Glu181^{EL2}, but only limited structural changes occur.[21] The Schiff base becomes deprotonated upon Meta IIa formation. Substantial structural changes occur with the subsequent formation of Meta IIb, including the TM6 movement first identified by EPR[22] and also seen in the crystal structures of opsin. Meta IIbH$^+$ formation is accompanied by a proton uptake reaction at the cytoplasmic surface, most likely by protonation of Glu134$^{3.49}$.[23] Infrared absorption bands could now be assigned to the transitions between the Meta states, corresponding to the microswitches that operate in the course of rhodopsin photoactivation.[24]

Tyr223$^{5.58}$ is part of a Y$^{5.58}$X$_7$K(R)$^{5.66}$ motif near the cytoplasmic end of TM5.[4] A recent NMR investigation of this region in mutant rhodopsins came to the conclusion that tyrosine at position 223 has a stabilizing effect on the active state of the receptor.[10] In the present paper, we extend these studies to specify the role of Tyr223$^{5.58}$ in the formation of the Meta intermediates (Scheme 1) and in the coupling to the G-protein. We have investigated the mutants Y223A (in which the bulky side chain of Tyr is lacking), Y223F (with a bulky aromatic side chain), and Y223E (with a polar side chain). By means of intrinsic G_t fluorescence measurements we have found that all of these mutants have reduced catalytic activity compared to wild-type, with the most dramatic reduction for the Y223A mutation. To elucidate the molecular background of this deficiency we applied UV−vis and FTIR difference spectroscopy to wild-type rhodopsin and Tyr223$^{5.58}$ mutants reconstituted in phospholipid vesicles to simulate a native environment in which all intermediates in Scheme 1 appear. While UV−vis spectroscopy of the Meta states reports mainly on the protonation state of the retinal Schiff base, FTIR difference spectroscopy allows us to identify structural changes beyond the direct protein chromophore interactions on a molecular level and under various conditions. We show how Tyr223$^{5.58}$, which is already involved in Meta I formation, comes into play with the formation of Meta IIb. In this step, it assists the breakage of the hydrogen-bond network between Arg135$^{3.50}$ and Glu247$^{6.30}$/Thr251$^{6.34}$. Postponed and along with proton uptake in Meta IIbH$^+$, the new interaction between Tyr223$^{5.58}$ and Arg135$^{3.50}$ is built up. The crystal structures of opsin and of the reversibly formed Meta II are in line with this spectroscopic characterization of the active species.[8,11,12] So the present study provides valuable information on binding site formation of the prominent class A GPCR rhodopsin.

MATERIALS AND METHODS

Sample Preparation. Rhodopsin mutants were prepared as described before.[25] During the last step of elution *n*-D-dodecyl-β-maltoside (DDM) buffer was changed to *n*-D-octyl-β-D-glucopyranoside for reconstitution into lipid vesicles that were used for FTIR-sandwich samples. Egg-PC (Avanti Polar Lipids Inc., Alabaster) was lyophilized and suspended in buffer A (20 mM BTP, 130 mM NaCl, 1 mM $MgCl_2$) to a concentration of 3 mg/mL. The suspension was then treated with five freeze−thaw cycles with liquid nitrogen and lukewarm water and extruded repeatedly through a 200 nm polycarbonate membrane. Subsequently, the suspension was incubated with purified rhodopsin in a molar ratio of 100:1 (lipid:protein)

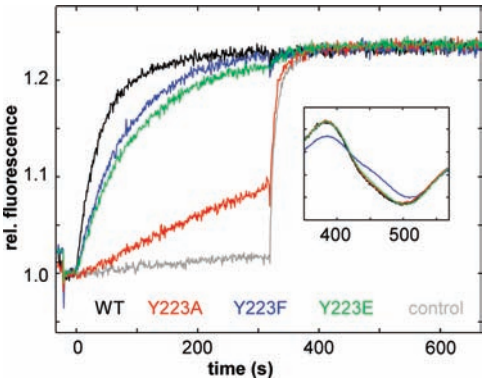

Figure 2. G-protein activation assay. The G-protein activation capacity of purified wild-type rhodopsin and of the Y223A, Y223F, and Y223E mutants determined by monitoring time-resolved tryptophan fluorescence changes in the G-protein resulting from GTPγS uptake at 20 °C and pH 6. The G_t activation rates are 100% (wild-type), 46% (Y223F), 41% (Y223E), and 6% (Y223A). Y223F does not show complete conversion to Meta II (inset). This suggests an even higher activation rate for Y223F-Meta II.

at 4 °C for 1 h. Thereafter the samples were dialyzed against 0.5 L of buffer A with 1 mM DTT and 2 g of Calbiosorb adsorbant (Merck, Germany) for 5 days at 10 °C by daily buffer exchange. Sandwich samples were prepared without any drying, as described earlier.[26] To achieve complex formation with the G-protein derived peptide CTα [G_tα(340−350)K341L, NH_2−ILENLKDCGLF−COOH] a 10 mM solution was added to the protein sample before centrifugation to reach a final concentration of 5 mM CTα peptide.

Coupled UV−Vis and FTIR Spectroscopy. An OLIS Rsm16 UV−vis spectrophotometer was coupled to the Bruker ifs66v/s FTIR spectrometer via fiberoptics to collect absorbance spectra in the region 350−570 nm and FTIR difference spectra in parallel. Illumination was performed with LEDs for 3 s with λ_{max} = 530 nm at 30 °C or 10 s with λ_{max} = 590 nm at 0 °C to prevent formation of isorhodopsin, which can form by photolysis of the Lumi and Meta I intermediate.

Activation Measurements. To determine receptor activity, we use the intrinsic tryptophan fluorescence assay.[27] Activity can only properly be determined in detergent, because in lipid vesicles other rate-limiting steps, such as the association of soluble G_t with the membrane, become rate-limiting.[28] Furthermore, in vesicles the Meta I/Meta II ratio is strongly shifted toward Meta I for Y223F,[10] so it is impossible to obtain adequate amounts of Meta II for determination of the activation rate. At pH 6 we mixed 1.5 nM of solubilized receptor protein (0.006% DDM[29]) and 600 nM G_t with 5 μM GTPγS and triggered nucleotide exchange by 10 s illumination with λ > 540 nm. After 6 min, excess light-activated wild-type rhodopsin is added to activate all G_t present in the sample. The traces are normalized to the total amount of G_t, and the apparent activation rates are given by the initial slope calculated by least-squares fits. The gray line represents a control measurement without receptor; the other traces are corrected for this spontaneous G_t activity.

Data Processing. The calculated time-dependent FTIR absorbance difference spectra are analyzed by a specially designed combination of singular value decomposition and global analysis to increase signal-to-noise ratio.[26] The fastest component is usually taken for further analysis, while slower components are related to the decay process and sample instability. All spectra (except pH 8, 0 °C) that contain Meta I are corrected for this amount of Meta I. The amount was estimated by least-squares fits of the FTIR region between 1050 and 940 cm^{-1} to pure Meta I and Meta $IIbH^+$ spectra or by the 480 nm UV−vis absorbance. In other words, we first subtracted the Meta I fraction to eliminate the mutant-specific pK_a shift of the Meta I/Meta II equilibrium, to calculate afterward the mutants minus wild-type double difference spectrum (see Supporting Information Figure 1). Insets show the corresponding UV−vis difference spectrum photoproduct minus dark state without any further processing.

RESULTS

G-Protein Activation by Wild-Type and Tyr223 Mutants. In a first experiment (Figure 2), the catalytic activity of purified recombinant rhodopsin and of the Y223A, Y223F, and Y223E mutants was determined by monitoring the intrinsic tryptophan fluorescence change in the G-protein resulting from GTPγS uptake.[27] To exclude the influence of the lipid environment on the equilibrium between active and inactive species, we performed the experiments in detergent micelles in which for wild-type rhodopsin the Meta equilibria are completely shifted toward Meta IIb/Meta $IIbH^+$ (for details, see Materials and Methods). We find 6%, 41%, and 46% of the wild-type activation rate for Y223A, Y223E, and Y223F, respectively. Obviously, the Y223F mutant still exhibits 40% of a 480 nm absorbing species under these conditions (Figure 2, inset). This suggests that the actual activation rate is even higher than the apparent rate when only the Y223F-Meta II species are considered (up to 65% of wild-type activity).

FTIR Spectroscopy of $Tyr223^{5.58}$ Mutants at pH 8 and 0 °C. In order to elucidate the molecular reasons for the reduced catalytic activity, the impact of $Tyr223^{5.58}$ mutation on the Meta intermediates was investigated by FTIR difference spectroscopy. We recorded the illuminated state minus dark state FTIR difference spectrum of wild-type rhodopsin at pH 8 and 0 °C and of the Y223A, Y223F, and Y223E mutants under identical conditions (Figure 3A and Supporting Information Figure 2A) and calculated the double difference spectra (for detailed information, see methods section and Supporting Information Figure 1). The photoproduct minus dark state difference spectra of the mutants are shown as gray lines for direct comparison, and the respective UV−vis difference spectra are given as insets. Neither the 500 nm dark state absorption maximum nor the 480 nm absorption of the Meta I intermediate is significantly influenced by the mutations.

Alterations at $^{+}1745/^{-}1720$ and $^{+}1236$ cm^{-1} are revealed by the FTIR double difference spectra indicating small differences between wild-type Meta I and the photoproduct of the mutants (superscripted + or − denotes the orientation of the band). All mutants show very similar deviations from wild-type, and H_2O to D_2O exchange does not affect these bands (Supporting Information Figure 3).

Meta IIa and Meta IIb Formation at 30 °C, pH 8. Increasing the temperature to 30 °C leads to the formation of Meta IIa and Meta IIb at the expense of Meta I.[30] As seen in the UV−vis difference reflecting the Meta I/Meta II ratio (Figure 3B, insets), wild-type, Y223A, Y223F, and Y223E exhibit a ratio of 35:65, 35:65, 60:40, and 35:65, respectively. In wild-type rhodopsin, FTIR bands typical for Meta IIa ($^{-}1768$ and $^{+}1687$ cm^{-1}) and Meta IIb ($^{+}1745$, $^{-}1656$, and $^{+}1643$ cm^{-1}) monitor the fractions of these intermediates[24] (Figure 3B). Corresponding spectra were also recorded for the $Tyr223^{5.58}$ mutants. For better comparison of the Meta IIa and Meta IIb species, the specific amount of Meta I present in each sample was subtracted before the double differences were calculated. The original difference spectra are shown in Supporting Information Figure 2B.

We find only small deviations in the structurally sensitive amide I region ($^{+}1664$, $^{-}1643$ cm^{-1}) for Y223A, which most likely originate from different rotameric states of the $Tyr223^{5.58}$ side chain and their influence on the backbone vibration. Polar interactions of $Tyr223^{5.58}$

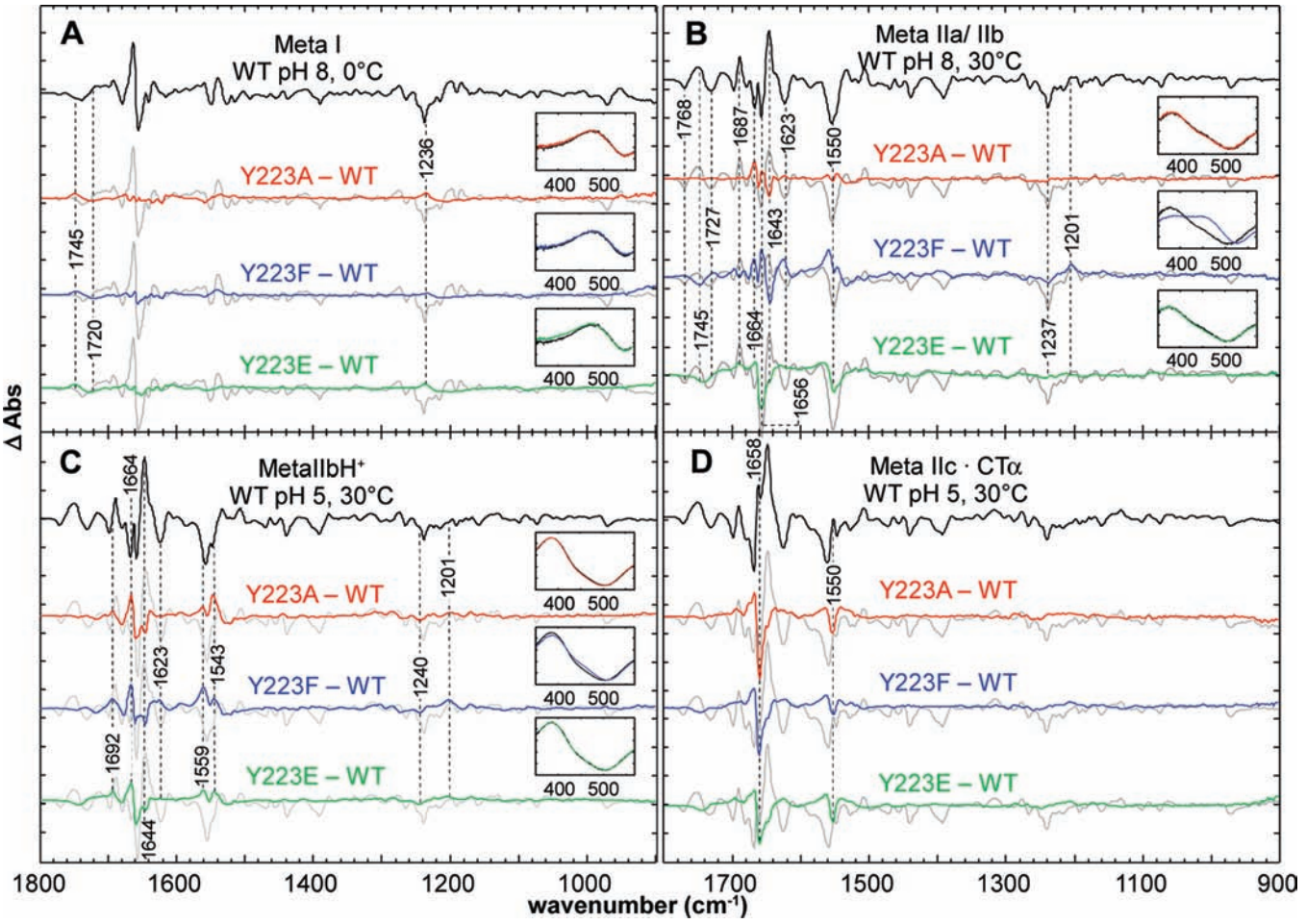

Figure 3. Coupled UV−vis and FTIR spectroscopy of wild-type and mutant photointermediates. (A) Wild-type and Y223A, Y223F, and Y223E minus wild-type double difference spectra recorded at pH 8, 0 °C (Meta I conditions), superimposed with the mutant Meta I differences (gray). The UV−vis difference spectra (insets) show a 500−480 nm transition, indicating a dark state to Meta I transition. The FTIR double difference spectra indicate small alterations introduced by the mutation of Tyr223$^{5.58}$. Interestingly, all mutants show very similar deviations compared to the wild-type. (B) The spectra recorded at 30 °C, pH 8, were corrected for Meta I content and therefore represent the dark state to Meta IIa/Meta IIb transition. The same experiment was performed with the mutants (gray), and subsequently the Y223A, Y223F, and Y223E minus wild-type double difference spectra were calculated. (C) Photoproduct minus dark state difference spectrum wild-type at pH 5, 30 °C, indicates the formation of Meta IIbH$^+$. The bands in the double differences represent structural deviations between wild-type Meta IIbH$^+$ and the respective photoproducts of the mutants. (D) Photoproduct minus dark state difference spectrum in the presence of CTα peptide recorded at 30 °C, pH 5 (Meta IIc). The mutants' Meta IIc state minus wild-type Meta IIc double difference spectra represent structural changes in the receptor/peptide complexes caused by the mutations (see Results section for detailed description).

are excluded since tyrosine/tyrosinate specific difference bands are lacking in the Y223A double difference. In contrast to this, Y223F mutation shifts the Meta equilibria toward Meta I, as indicated by the larger 480 nm absorption in the UV−vis difference spectrum. Specific alterations in the FTIR difference spectrum of this mutant are the double difference bands at $^{-}$1237/$^{+}$1201 cm^{-1} (retinal fingerprint region), a large positive band above 1550 cm^{-1}, several features in the amide I region between 1600 and 1700 cm^{-1}, and the band centered at $^{-}$1745 cm^{-1} (carbonyl stretching vibrations). However, the typical Meta IIa bands at $^{-}$1768 and $^{+}$1687 cm^{-1} exhibit intensities comparable to the wild-type, demonstrating that Y223F mutation does not directly influence Schiff base deprotonation. All Meta IIb characteristics have little if any intensity, showing that Meta IIb formation is impaired by this mutation. The strongly reduced bands at $^{+}$1745/$^{-}$1727 cm^{-1} have been assigned to changes of the TM3/TM5 network (cf. Figure 1A)[31] which occur in parallel with TM6 outward movement.[24] It seems likely that the large deviations in the carboxylate (above 1550 cm^{-1}) and fingerprint regions ($^{-}$1237/$^{+}$1201 cm^{-1}) reflect the inhibition of activating changes in the Glu247$^{6.30}$/Thr251$^{6.34}$ and Lys231$^{5.66}$ network depicted in the opsin structure in Figure 1C, the latter residue constituting the counterpart of Tyr$^{5.58}$ in the Y$^{5.58}$X$_7$K-(R)$^{5.66}$ motif. We note that Y223F depletes Meta IIb but not Meta IIa by blocking TM5 movement. This leads to a shift of the coupled equilibria to Meta I. The UV−vis difference spectrum of Y223E indicates the same ratio of Meta I/Meta II species as in Y223A and wild-type. Additional bands in the amide I and amide II region of the Y223E difference spectrum reflect even larger structural changes than observed with the wild-type ($^{-}$1656 and $^{-}$1550 cm^{-1}), most likely due to polar interactions of the carboxylate of Y223E in the rhodopsin dark state.

Meta IIbH$^+$ at 30 °C, pH 5. In Figure 3C we present the FTIR difference spectrum of wild-type rhodopsin recorded under conditions favoring Meta IIbH$^+$ formation. At this low pH no Meta I is formed in wild-type rhodopsin, and in the UV−vis spectral range only the absorption with maximum at 380 nm is observed

dx.doi.org/10.1021/ja200545n |J. Am. Chem. Soc. 2011, 133, 7159–7165

Scheme 2

Meta I ⇌ Meta IIa ⇌ Meta IIb ⇌ Meta IIbH$^+$

⇅

Meta IIC · CTα

(Figure 3C, inset). The same applies to the Y223A and Y223E mutants, while the Y223F still shows 10% Meta I. As for the other intermediates, this amount was subtracted for better comparison before calculation of the FTIR double differences. A very similar pattern of double difference bands in the amide I ($^+$1664/$^-$1658 and $^-$1644 cm^{-1}) and amide II (around 1550 cm^{-1}) regions is found for all mutants, suggesting a similar influence of all mutations on the structure of Meta IIbH$^+$. Y223F mutation leads to larger double difference bands at $^+$1692, $^+$1623, and $^+$1559 cm^{-1}, while Y223E mutation exhibits smaller differences, especially with respect to the amide I band at $^+$1644 cm^{-1}. The similarity of all double differences lets us conclude that under these low pH conditions, where Glu134$^{3.49}$ becomes protonated, Arg135$^{3.50}$ is released in all mutants from the intrahelical salt bridge.

FTIR Spectroscopy of the Meta IIc·CTα Complex. The high receptor protein concentration (~3 mM) in the sandwich samples used for FTIR spectroscopy makes it impossible to add stoichiometric amounts of G-protein for studies of receptor-G-protein coupling. Therefore, an 11-mer G-protein derived peptide, G$_t$α (340−350) K341L (CTα), was used, which is known to stabilize the active conformation similar to the holoprotein.[32,33] NMR investigations have detected a random coil to α-helix transition of the native G$_t$α(340−350) peptide upon complex formation.[34] In addition to the structuring in the CTα peptide, complex formation leads to conformational changes in the receptor protein.[35] The receptor intermediate that forms in the presence of the peptide represents the G-protein interacting species and is termed Meta IIc in the following.

Compared to Meta IIbH$^+$, the wild-type Meta IIc difference spectrum (Figure 3D) exhibits mainly two additional bands at $^+$1658 cm^{-1} (amide I) and $^+$1550 cm^{-1} (amide II). The sharp amide I band was assigned to structural changes of the receptor, indicating differences between Meta IIbH$^+$ and the CTα bound form. The amide II band comprises changes in both the receptor and peptide.[35] In the Meta IIc spectra of the mutants, the intensities of these bands are significantly reduced, as shown by the double difference bands at $^-$1658 and $^-$1550 cm^{-1}. These features appear clearly against the background of deficiencies of the mutant precursor states, which indicates that the structural deficiencies of Meta IIbH$^+$ are still present in Meta IIc. The intensity of these bands can by qualitatively correlated with the mutant activity, as measured by intrinsic fluorescence change (cf. Figure 1). The band at $^+$1658 cm^{-1} is least affected by Y223E mutation, whereas Y223F exhibits less deviations around 1550 cm^{-1}. The double difference band at $^+$1559 cm^{-1} present in Meta IIbH$^+$ of Y223F disappears upon CTα binding. This is exactly the region where the peptide structuring is monitored.[35] We conclude that the polar side chain of Y223E accomplishes the receptor structural changes at least partially, whereas the phenyl ring of Y223F suffices to induce α-helical structure in the CTα peptide. In both regions the Y223A mutation exhibits the largest differences to wild-type, demonstrating that Y223A cannot perform either of these tasks of Tyr223$^{5.58}$, which is in agreement with the largely reduced activity of this mutant.

DISCUSSION

The crystal structures of rhodopsin's active state[8,36] suggest a stabilizing role of Tyr223$^{5.58}$ in forming the CTα binding site by involving the guanidine side chain of Arg135$^{3.50}$ in a strong hydrogen bond. This interaction leads to a new orientation of the Arg135$^{3.50}$ side chain so that the unbound NH$_2$ of its guanidine group points toward the cytoplasmic surface, thereby eventually providing a hydrogen bond donor for binding of CTα. Y223F and Y223E show considerably higher activity toward the G-protein than the Y223A mutant, suggesting that both the hydroxyl group and the hydrophobic phenyl ring of the tyrosine phenol side chain codetermine the activity. Combining this information with UV−vis and FTIR spectroscopy enables us to investigate the development of binding site formation and G-protein coupling in molecular detail. Extending the three-step activation scheme of Meta intermediates (Scheme 1), the discussion of the results will be based on Scheme 2.

The Meta I State (Schiff Base Counterion Shift). The Meta I intermediate accumulating at low temperature (Figure 3A) and basic pH appears in all mutant rhodopsins with small but distinct deviations from wild-type. This indicates that neither the introduction of a polar side chain nor the presence of the phenyl ring is sufficient to restore a complete dark state to the Meta I transition. Already at this stage of the light-induced transduction path the signal is transmitted from the photosensory ligand to the cytoplasmic domain, in which Tyr223$^{5.58}$ is located. Therefore, we tentatively assign the band at $^+$1236 cm^{-1} to a tyrosine vibration of the mutated Tyr223$^{5.58}$ itself, since tyrosine is known to cause absorptions in this region which, as observed, may not be affected by deuteration.[37,38] The same insensitivity to H_2O/D_2O exchange is seen with the band at $^+$1745 /$^-$1720 cm^{-1}, which is thus most likely not due to a protein carbonyl but caused by a lipid ester group, as already reported for the transition to Meta II.[39] Since very similar differences are observed when Meta I is stabilized in detergent micelles,[31] we envisage an interaction between Tyr223$^{5.58}$ and a lipid molecule, which is changed in the Meta I state depending on a movement of TM5. This is in line with a recent FTIR study using azido-labeled side chains, which has proposed an outward movement of TM5 and rotation of TM6 as early as with Meta I formation.[40]

Formation of Meta IIa (Schiff Base Deprotonation). No significant impact of any of the mutations was detected on the step that follows on Meta I. The intensity of the Meta IIa marker bands (Figure 3B) is very similar in all mutants and wild-type, demonstrating that Schiff base deprotonation is not affected by the properties of the side chain at position 223. In agreement with earlier studies,[4] this step is not linked to major structural changes occurring around Tyr223$^{5.58}$.

Formation of Meta IIb (Gross Structural Changes). In Meta IIb, TM6 is released from the helical bundle,[18] and the interactions between Glu247$^{6.30}$/Thr251$^{6.34}$ and Arg135$^{3.50}$ are broken. This most significant conformational conversion in the activation process results in the cleft between TM3/5 and TM6, thus providing a binding site for the G$_t$ α-subunit.[12] When Tyr223$^{5.58}$ is exchanged against alanine, the intensities of the Meta IIb typical FTIR bands (Figure 3B) are only slightly influenced and the Meta I/Meta II ratio remains the same. This shows that the Tyr223$^{5.58}$ side chain is not unconditionally needed to induce breakage of the Glu247$^{6.30}$−Arg135$^{3.50}$−Thr251$^{6.34}$ network, which leads to TM6 outward movement. The spectroscopic features collectively indicate that TM3, TM5, TM6 remain in their inactive

dx.doi.org/10.1021/ja200545n |J. Am. Chem. Soc. 2011, 133, 7159–7165

arrangement in Y223F. Conceivably, without the phenol OH group the bulky, apolar phenyl ring is not capable of entering the polar environment around Arg135$^{3.50}$. Also other factors may influence the in/out equilibrium of the side chain at position 223: Tyrosine is known to "snorkel"[41] in the lipid bilayer surrounding the membrane protein, and the lack of the OH group means a dramatic change in this property. Eventually, TM5 is hindered to adopt its active, inward tilted conformation, leading to the notion that early structural alterations of TM5 are a prerequisite for TM6 outward movement and also for the formation of the hydrogen bond network involving Glu247$^{6.30}$, Thr251$^{6.34}$, and Lys231$^{5.66}$ (cf. Figure 1 C). In turn, we conclude that in Meta IIb the Tyr223$^{5.58}$ side chain enters the environment around Arg135$^{3.50}$ to provide an acceptor for the guanidinium group.

Formation of Meta IIbH$^+$ (Proton Uptake). Tyr223$^{5.58}$ mutation has a strong impact on this process, which is linked to the uptake of a proton from the cytoplasm. The data clearly indicate that all mutants exhibit very similar defects in this state. We conclude that only the complete phenol side chain of Tyr223$^{5.58}$ is able to bind Arg135$^{3.50}$ via hydrogen bond, and this occurs when the salt bridge between Arg135$^{3.50}$ and Glu134$^{3.49}$ is broken. Thus, the pK_a of proton uptake by Glu134$^{3.49}$ is decisively defined by the molecular characteristics of Tyr223$^{5.58}$. In line with the two crystal structures of active opsin and of the reversibly formed Meta II, this interaction remains intact also in the subsequent transition to Meta IIc.[8,11,12] The two constituents, Tyr223$^{5.58}$ and Lys231$^{5.66}$, of the Y$^{5.58}$X$_7$K(R)$^{5.66}$ motif appear to stabilize the active helical arrangement. Both do not adopt their active conformation in the Y223F mutant, resulting in the strong shift to Meta I. This does not apply for the other mutants, where the TM5 inward movement occurs and at least the Glu247$^{6.30}$−Lys231$^{5.66}$ lock can form.

Formation of Meta IIc (G-Protein Interaction). G_t or CTα peptide stabilizes the Meta IIc intermediate by a hydrogen bond between Arg135$^{3.50}$ and the backbone carbonyl of Cys347$^{CT\alpha}$. Unfortunately, receptor activity and the FTIR bands reflecting the underlying structural conversions cannot be quantitatively correlated because of the difference in the measuring system (detergent solution vs lipid vesicles). We observe the most significant structural deviations between the mutants and the wild-type for the mutant with the lowest activity (Y223A). Also the relatively high activities of Y223E and Y223F can also be explained at least qualitatively: the Y223E can provide in part the orientation and stabilization of Arg135$^{3.50}$, while the phenyl group of Y223F is able to build up hydrophobic interactions with the G-protein. A decisive role of hydrophobic interactions is also consistent with the high affinity of peptide analogs, in which polar residues are replaced with hydrophobic ones.[42,43] Available structural information of the opsin−CTα complex also emphasizes the role of hydrophobic contacts and suggests that the corresponding entropy gain may provide a large contribution for efficient signal transduction.

CONCLUSION

The salient result of this study is that the distinctive side chain characteristics of a highly conserved residue play a decisive role for different steps during the activation process of the prototypical class A GPCR rhodopsin and for subsequent signal transfer to the G-protein. We have seen that the complete lack of a side group ring system allows the activating conformational changes to proceed to the last of the Meta intermediates, but the receptor fails to activate its G-protein because of the lack of hydrophobic interactions. The phenyl moiety alone without the hydroxyl group provides large hydrophobic interaction capacity but strongly impairs opening of the binding site. The hydroxyl group is involved in the stabilizing interaction with Arg135$^{3.50}$ and comes into play in concert with the proton uptake reaction. The phenol side chain of tyrosine provides all features, the capability to accumulate the active state, the polarity to ensure the proper active conformation, and the bulky hydrophobic ring system required for efficient G-protein activation. It is likely that the high conservation of Tyr223$^{5.58}$ among class A GPCRs[10] is based on the unique combination of these features.

ASSOCIATED CONTENT

Supporting Information. FTIR results and one methodical figure. This material is available free of charge via the Internet at http://pubs.acs.org.

AUTHOR INFORMATION

Corresponding Author

franz.bartl@charite.de; klaus_peter.hofmann@charite.de; matthias.elgeti@charite.de

Present Addresses

[⊥]Department of Biochemistry, University of Toronto, 1 King's College Circle, Toronto, Ontario M5S 1A8, Canada.

[±]Departments of Biochemistry and Molecular Genetics, University of Toronto, 1 King's College Circle, Toronto, Ontario M5S 1A8, Canada.

[¶]Institut für Molekulare Medizin and Zellforschung, Sektion Biophysik, Albert-Ludwig-Universität Freiburg, Freiburg, Germany.

Author Contributions

[‖]These authors contributed equally.

ACKNOWLEDGMENT

We thank Ingrid Semjonow, Jana Engelmann, Anja Koch, Brian Bauer, Andreas v. Garnier, and Thomas Penczok for technical assistance. Financial support came from DFG (SFB498 to F.J.B. and K.P.H., SFB740 to O.P.E., M.H., and K.P.H.) and ERC (Advanved Grant to K.P.H.).

REFERENCES

(1) Rosenbaum, D. M.; Rasmussen, S. G. F.; Kobilka, B. K. *Nature* **2009**, *459*, 356–363.

(2) Ballesteros, J. A.; Weinstein, H. *Methods Neurosci.* **1995**, *25*, 366–428.

(3) Lin, S. W.; Han, M.; Sakmar, T. P. *Methods Enzymol.* **2000**, *315*, 116–130.

(4) Hofmann, K. P.; Scheerer, P.; Hildebrand, P. W.; Choe, H.-W.; Park, J. H.; Heck, M.; Ernst, O. P. *Trends Biochem. Sci.* **2009**, *34*, 540–552.

(5) Nygaard, R.; Frimurer, T. M.; Holst, B.; Rosenkilde, M. M.; Schwartz, T. W. *Trends Pharmacol. Sci.* **2009**, *30*, 249–259.

(6) Li, J.; Edwards, P. C.; Burghammer, M.; Villa, C.; Schertler, G. F. X. *J. Mol. Biol.* **2004**, *343*, 1409–1438.

(7) Vogel, R.; Mahalingam, M.; Lüdeke, S.; Huber, T.; Siebert, F.; Sakmar, T. P. *J. Mol. Biol.* **2008**, *380*, 648–655.

(8) Choe, H.-W.; Kim, Y. J.; Park, J. H.; Morizumi, T.; Pai, E. F.; Krauss, N.; Hofmann, K. P.; Scheerer, P.; Ernst, O. P. *Nature* **2011**, *471*, 651–655.

(9) Vogel, R.; Siebert, F. *J. Biol. Chem.* **2001**, *276*, 38487–38493.

(10) Goncalves, J. A.; South, K.; Ahuja, S.; Zaitseva, E.; Opefi, C. A.; Eilers, M.; Vogel, R.; Reeves, P. J.; Smith, S. O. *Proc. Natl. Acad. Sci. U. S. A.* **2010**, 38–40.
(11) Park, J. H.; Scheerer, P.; Hofmann, K. P.; Choe, H.-W.; Ernst, O. P. *Nature* **2008**, *454*, 183–187.
(12) Scheerer, P.; Park, J. H.; Hildebrand, P. W.; Kim, Y. J.; Krausz, N.; Choe, H.-W.; Hofmann, K. P.; Ernst, O. P. *Nature* **2008**, *455*, 497–502.
(13) Cherfils, J.; Chabre, M. *Trends Biochem. Sci.* **2003**, *28*, 13–17.
(14) Oldham, W. M.; Van Eps, N.; Preininger, A. M.; Hubbell, W. L.; Hamm, H. E. *Nat. Struct. Mol. Biol.* **2006**, *13*, 772–777.
(15) Scheerer, P.; Heck, M.; Goede, A.; Park, J. H.; Choe, H.-W.; Ernst, O. P.; Hofmann, K. P.; Hildebrand, P. W. *Proc. Natl. Acad. Sci. U. S. A.* **2009**, *106*, 10660–10665.
(16) Emeis, D.; Kühn, H.; Reichert, J.; Hofmann, K. P. *FEBS Lett.* **1982**, *143*, 29–34.
(17) Matthew, R. G.; Hubbard, R.; Brown, P. K.; Wald, G. *J. Gen. Physiol.* **1963**, *47*, 215–240.
(18) Knierim, B.; Hofmann, K. P.; Ernst, O. P.; Hubbell, W. L. *Proc. Natl. Acad. Sci. U. S. A.* **2007**, *104*, 20290–20295.
(19) Deupi, X.; Kobilka, B. K. *Physiology (Bethesda, MD)* **2010**, *25*, 293–303.
(20) Okada, T.; Ernst, O. P.; Palczewski, K.; Hofmann, K. P. *Trends Biochem. Sci.* **2001**, *26*, 318–324.
(21) Lüdeke, S.; Beck, M.; Yan, E. C. Y.; Sakmar, P. T.; Siebert, F.; Vogel, R. *J. Mol. Biol.* **2005**, *353*, 345–356.
(22) Farrens, D. L.; Altenbach, C.; Yang, K.; Hubbell, W. L.; Khorana, H. G. *Science* **1996**, *274*, 768–770.
(23) Arnis, S.; Fahmy, K.; Hofmann, K. P.; Sakmar, T. P. *J. Biol. Chem.* **1994**, *269*, 23879–23881.
(24) Zaitseva, E.; Brown, M. F.; Vogel, R. *J. Am. Chem. Soc.* **2010**, *132*, 4815–4821.
(25) Fritze, O.; Filipek, S.; Kuksa, V.; Palczewski, K.; Hofmann, K. P.; Ernst, O. P. *Proc. Natl. Acad. Sci. U. S. A.* **2003**, *100*, 2290–2295.
(26) Elgeti, M.; Ritter, E.; Bartl, F. J. *Z. Phys. Chem.* **2008**, *222*, 1117–1129.
(27) Fahmy, K.; Sakmar, T. P. *Biochemistry* **1993**, *32*, 7229–7236.
(28) Ernst, O. P.; Bieri, C.; Vogel, H.; Hofmann, K. P. *Methods Enzymol.* **2000**, *315*, 471–489.
(29) Ernst, O. P.; Gramse, V.; Kolbe, M.; Hofmann, K. P.; Heck, M. *Proc. Natl. Acad. Sci. U. S. A.* **2007**, *104*, 10859–10864.
(30) Mahalingam, M.; Martínez-Mayorga, K.; Brown, M. F.; Vogel, R. *Proc. Natl. Acad. Sci. U. S. A.* **2008**, *105*, 17795–17800.
(31) Beck, M.; Sakmar, T. P.; Siebert, F. *Biochemistry* **1998**, *37*, 7630–7639.
(32) Hamm, H. E.; Deretic, D.; Arendt, A.; Hargrave, P. A.; Koenig, B.; Hofmann, K. P. *Science* **1988**, *241*, 832–835.
(33) Herrmann, R.; Heck, M.; Henklein, P.; Henklein, P.; Kleuss, C.; Hofmann, K. P.; Ernst, O. P. *J. Biol. Chem.* **2004**, *279*, 24283–24290.
(34) Kisselev, O. G.; Kao, J.; Ponder, J. W.; Fann, Y. C.; Gautam, N.; Marshall, G. R. *Proc. Natl. Acad. Sci. U. S. A.* **1998**, *95*, 4270–4275.
(35) Vogel, R.; Martell, S.; Mahalingam, M.; Engelhard, M.; Siebert, F. *J. Mol. Biol.* **2007**, *366*, 1580–1588.
(36) Standfuss, J.; Edwards, P. C.; D'Antona, A.; Fransen, M.; Xie, G.; Oprian, D. D.; Schertler, G. F. X. *Nature* **2011**, *471*, 656–660.
(37) Gerothanassis, I. P.; Birlirakis, N.; Sakarellos, C. *J. Am. Chem. Soc.* **1992**, 9043–9047.
(38) DeLange, F.; Klaasen, C. H.; Wallace-Williams, S. E.; Bovee-Geurts, P. H. M.; Liu, X.; DeGrip, W. J.; Rothschild, K. J. *J. Biol. Chem.* **1998**, *273*, 23735–23739.
(39) Beck, M.; Siebert, F.; Sakmar, T. P. *FEBS Lett.* **1998**, *436*, 304–308.
(40) Ye, S.; Zaitseva, E.; Caltabiano, G.; Schertler, G. F. X.; Sakmar, T. P.; Deupi, X.; Vogel, R. *Nature* **2010**, *464*, 1386–1389.
(41) Liang, J.; Adamian, L.; Jackups, R. *Trends Biochem. Sci.* **2005**, *30*, 355–357.
(42) Martin, E. L.; Rens-Domiano, S.; Schatz, P. J.; Hamm, H. E. *J. Biol. Chem.* **1996**, *271*, 361–366.
(43) Janz, J. M.; Farrens, D. L. *J. Biol. Chem.* **2004**, *279*, 29767–29773.